TAB 1

CAPILLARY ELECTROPHORESIS

THEORY AND PRACTICE

Edited by
PAUL D. GROSSMAN • JOEL C. COLBURN

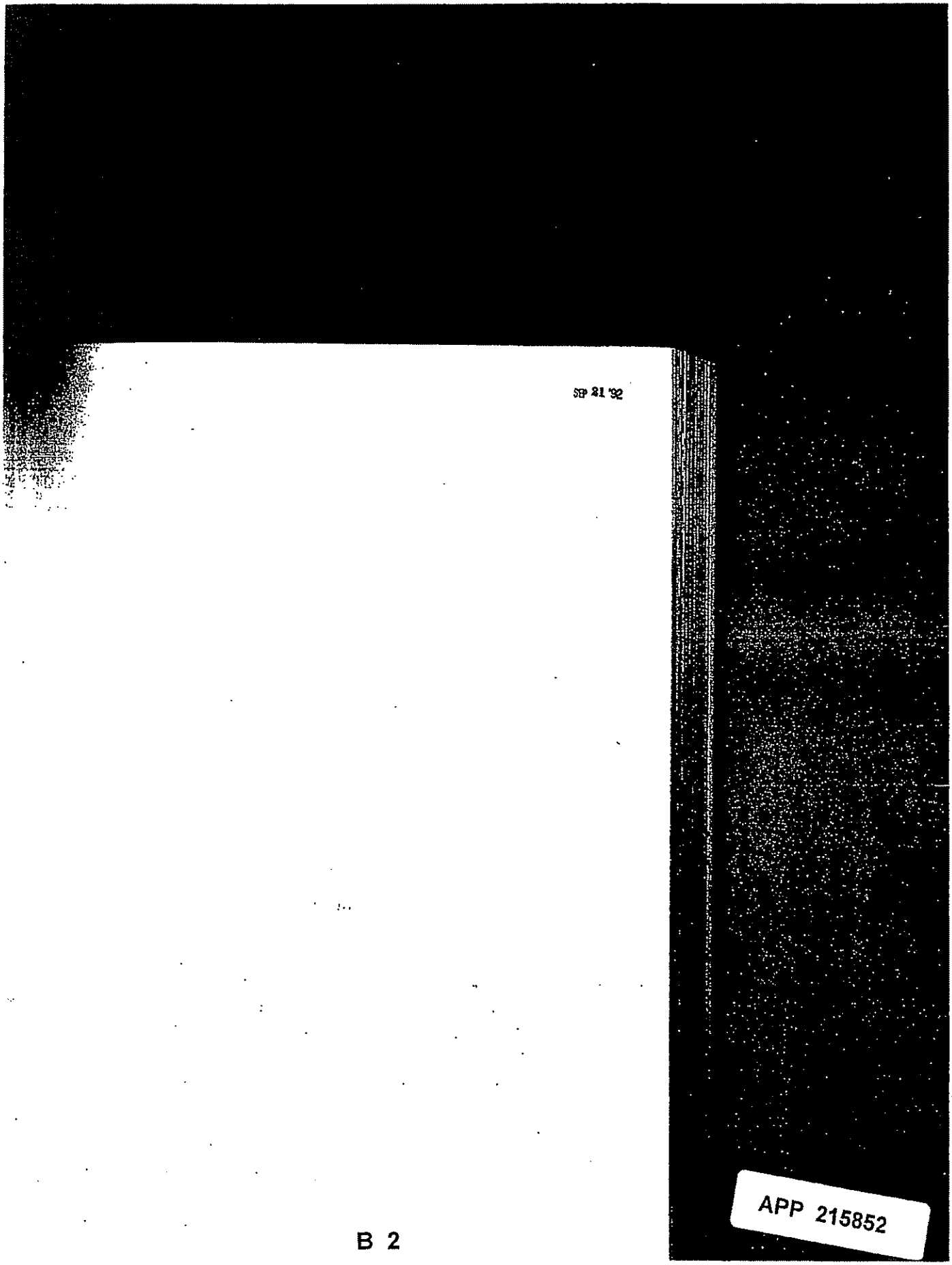

B 2

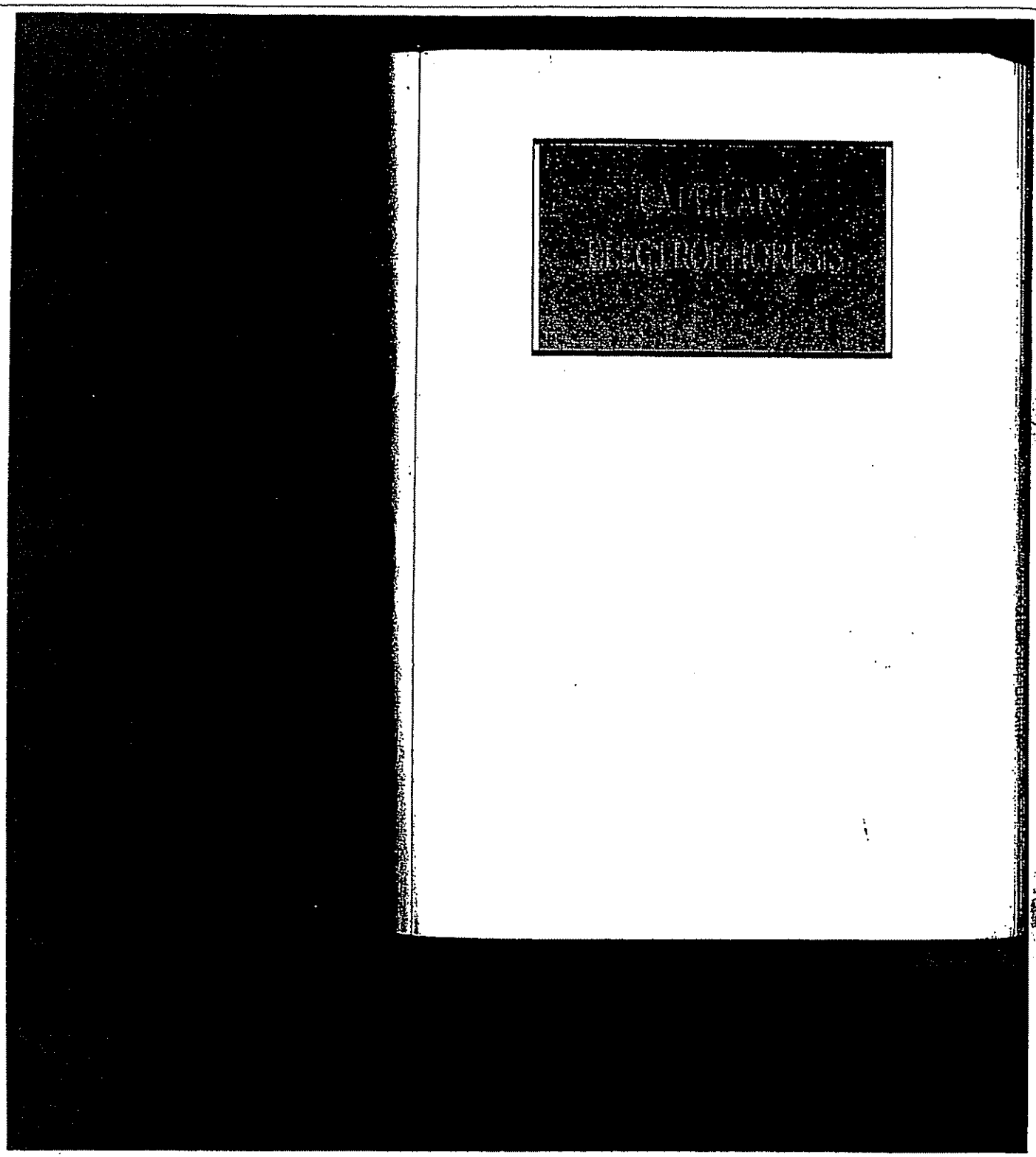
CALGARY
REGISTRATION

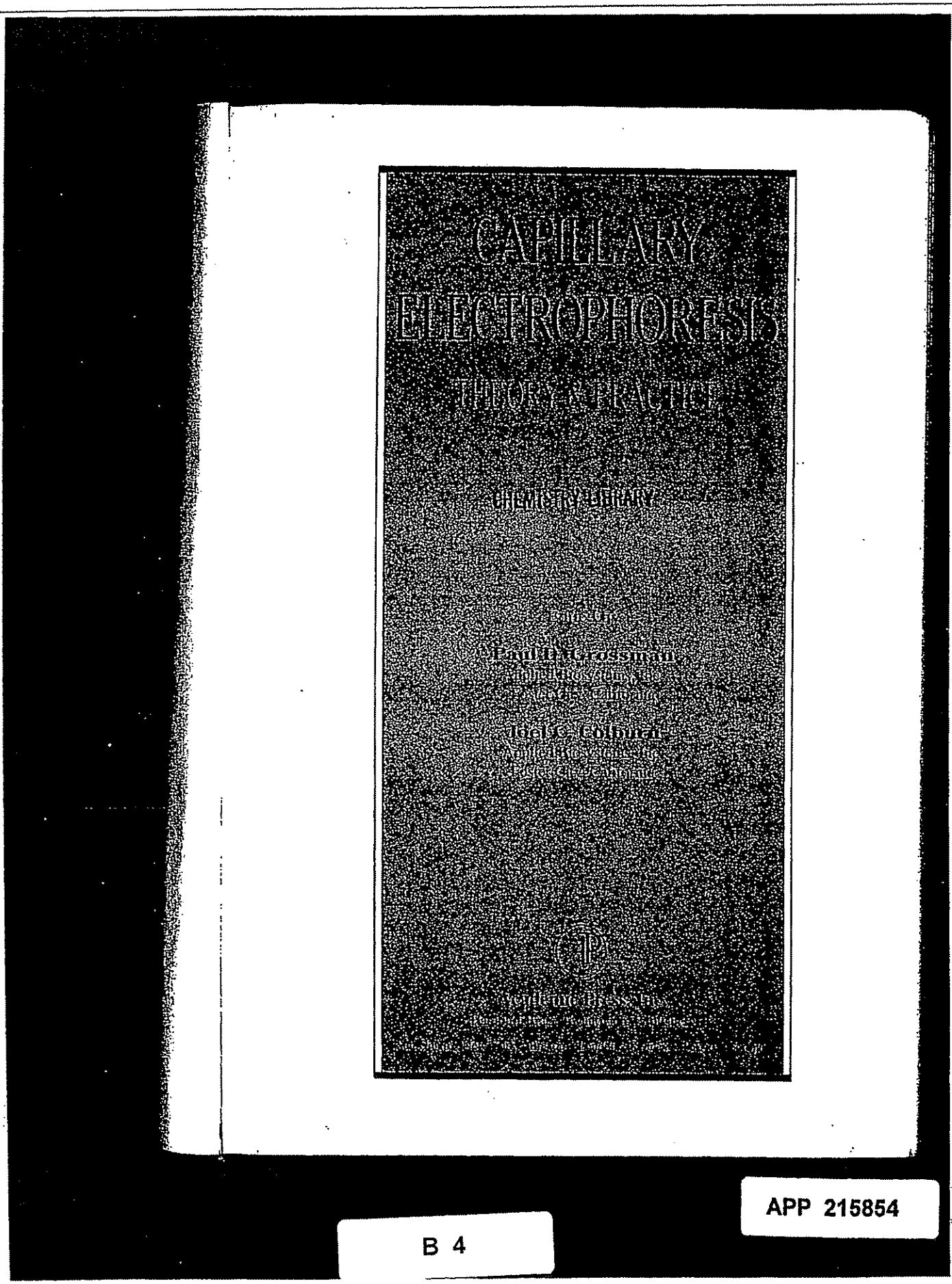

This book is printed on acid-free paper. ♾

Academic Press, Inc.
1250 Sixth Avenue, San Diego, California 92101-4311

United Kingdom Edition published by
Academic Press Limited
24–28 Oval Road, London NW1 7DX

Library of Congress Cataloging-in-Publication Data

Capillary electrophoresis : theory & practice / edited by Paul D. Grossman and Joel C. Colburn.
p. cm.
Includes bibliographical references and index.
ISBN 0-12-304250-X
1. Capillary electrophoresis. I. Grossman, Paul D. II. Colburn, Joel C.
QP519.9.C36C37 1992
574.19'285--dc20 92-6481
CIP

PRINTED IN THE UNITED STATES OF AMERICA
92 93 94 95 96 97 BC 9 8 7 6 5 4 3 2 1

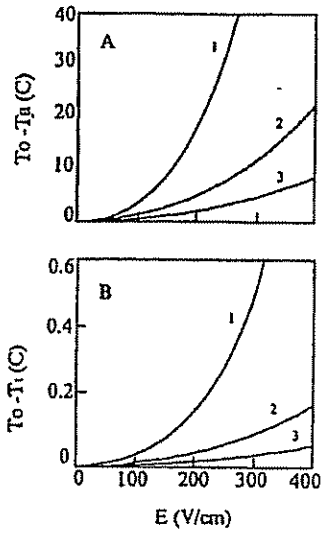

Figure 6 Calculated curves showing $T_0 - T_s$ and $T_0 - T_t$ as a function of electrical field strength for 3 different buffers. The curves were generated using Eqs. (13) and (17). The buffers used were the same as those in Fig. 3: (1) 100 m*M* sodium phosphate, pH 7.0; (2) 50 m*M* sodium citrate, pH 2.5; (3) 20 m*M* [cyclohexylamino] propanesulfonic acid (CAPS), pH 11.0.

400 V/cm. In this case, from Eq. (7), $T_0 - T_1 = 0.182°C$ (e.g., $\Delta T/\Delta r \cdot 7280°C/m$) and $\Delta\rho/\Delta T(\text{water}) \approx 0.221$ kg/m^3 °C. Recognizing that $\Delta\rho/\Delta r = \Delta T/\Delta r \cdot \Delta\rho/\Delta T$, Eq. (1) predicts a value for Ra of $4.3 \cdot 10^{-5}$. Thus, convective mixing is not an issue in this case.

III. Electroosmosis

Electroosmosis (EO) is the bulk flow of liquid due to the effect of the electric field on counterions adjacent to the negatively charged capillary wall. Because the wall of the fused-silica capillary is negatively charged at most pH conditions, there is a build-up of positive counterions in the solution adjacent to the capillary wall. When an electric field is applied, this layer of positive charge is drawn toward the negative electrode, resulting in the bulk flow of liquid toward that electrode.

Electroosmosis is present to some degree in all electrophoresis formats, but it is particularly important in CE. This is because of the high surface-area-to-volume ratio, the low viscosity of the electrophoresis medium, and the very high electric fields used in CE. A brief theoretical discussion follows of the mechanisms underlying EO and practical methods that have been developed to control it.

A. The Electrical Double Layer

The first step in describing EO is to quantitatively describe the charge density of counterions in solution near the capillary wall. This counter-ion-rich region is called the electrical double layer. The following treatment follows closely that of Hiemenz (1986).

The charge density of ions in solution, $\rho_e(x)$, where x is the distance from the capillary wall, is related to the ion concentration by the expression,

$$\rho_e(x) = \sum_i z_i e n_i(x) \tag{23}$$

where z_i is the valence of each ion, e is the charge on an electron, $n_i(x)$ is the number of ions of type i per unit volume near the capillary surface, and the sum is over all ions in the solution. In this analysis we will assume that n_i is a function of x only. Thus, in order to find $\rho_e(x)$, we must find an expression for $n_i(x)$.

Debye and Hükel proposed that the number density of ions in solution near a charged surface is determined by the competition between electrostatic attraction (or repulsion) of the ions for the charged interface and the randomizing influence of Brownian motion. This relationship is expressed in terms of a Boltzmann distribution, where

$$\frac{n_i(x)}{n_{i0}} = \exp\left(\frac{-z_i e \psi(x)}{kT}\right) \tag{24}$$

where n_{i0} is the number of ions per unit volume at a point of zero potential, $\psi(x)$ is the electrical potential at position x, k is Boltzmann's constant and T is the absolute temperature. Combining Eqs. (23) and (24) gives $\rho_e(x)$ as a function of the properties of the ions in solution and $\psi(x)$,

$$\rho_e(x) = \sum_i z_i e n_{i0} \exp\left(\frac{-z_i e \psi(x)}{kT}\right) \tag{25}$$

At this point an important assumption is made in order to simplify the further analysis. This assumption, known as the Debye-Hückel approximation, states that if $z_i e \psi(x) < kT$, the exponential term in Eq. (25) may be expanded into a power series truncated after the first-order terms [i.e., $e^x = (1 - x)$]. Inserting this approximate expression for the exponential term into Eq. (25) gives

$$\rho_e(x) = \sum_i \left(z_i e n_{i0} - \frac{z_i^2 e^2 n_{i0} \psi(x)}{kT}\right) \tag{26}$$

Because of the requirement for electroneutrality, the terms $\sum z_i e n_{i0}$ cancel from the

above summation, so that Eq. (26) reduces to

$$\rho_e(x) = \sum_i \frac{z_i^2 e^2 n_{i0}}{kT} \psi(x) \tag{27}$$

To find an explicit expression for $\rho_e(x)$, we need another expression relating $\psi(x)$ to $\rho_e(x)$. This equation is Poisson's equation, which gives the electrical potential as a function of the charge density. Because we are considering only the variation of ρ_e in the x direction, Poisson's equation reduces to

$$\frac{d^2\psi}{dx^2} = \frac{\rho_e(x)}{\varepsilon} \tag{28}$$

where ε is the electrical permittivity of the solvent. (The permittivity of a material is the constant, ε, in Coulomb's inverse square law, $F = q_1 q_2 / 4\pi\varepsilon r^2$, where F is the force between charges q_1 and q_2 separated by a distance r. The value of ε is given by the expression $\varepsilon = \varepsilon_0 \varepsilon_r$ where ε_0 is the permittivity of a vacuum, $8.854 \cdot 10^{-12}$ C^2 N^{-1} m^{-2}, and ε_r is the relative permittivity, or dielectric constant, of the medium; 78.54 for water at 25°C.) Thus, substituting Eq. (27) into Eq. (28) gives

$$\frac{d^2\psi}{dx^2} = \sum_i \frac{z_i^2 e^2 n_{i0}}{\varepsilon kT} \psi(x) \tag{29}$$

resulting in an explicit expression for $\psi(x)$. At this point, the grouping of constants in the sum in Eq. (29) are combined into a single constant, κ^2, where

$$\kappa^2 = e^2 \sum_i \frac{z_i^2 n_{i0}}{\varepsilon kT} \tag{30}$$

Thus, Eq. (29) becomes simply

$$\frac{d^2\psi}{dx^2} = \kappa^2 \psi(x) \tag{31}$$

The physical significance of κ^2 will be discussed shortly. Equation (31) can now be easily solved for $\psi(x)$ by integrating twice, using the boundary conditions: (1) $\psi = \psi_0$ when $x = 0$; (2) $\psi = 0$ when $x = \infty$, where ψ_0 is the electrical potential at the capillary–solution interface. The result of these integrations is

$$\psi(x) = \psi_0 \exp(-\kappa x) \tag{32}$$

Thus, as one moves away from the capillary wall, the electrical potential falls off exponentially, with a decay constant of κ. See Fig. 7. Finally, we are at the point where

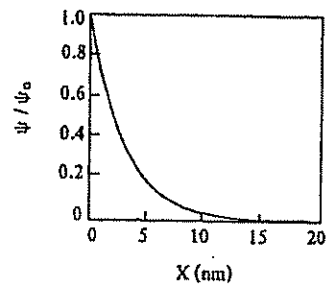

Figure 7 Plot of the electrical potential, ψ, as a fraction of the surface potential, ψ_0, as a function of the distance from the capillary wall, x. This curve was generated using Eq. (31) where a value of $3.29 \cdot 10^8$ m was used for κ (see Table I).

we can find an explicit expression for $\rho_e(x)$. Substituting Eq. (32) into Eq. (27) we obtain,

$$\rho_e(x) = \kappa^2 \psi_0 \exp(-\kappa x) \tag{33}$$

Thus given a value for κ, a property of the electrolyte solution, and a value for ψ_0, a property of the capillary wall, one can compute the charge density, $\rho_e(x)$, as a function of distance from the capillary wall.

At this point, it is important to make some observations regarding Eq. (33). First, with respect to the assumption of low electrical potential at the solution–capillary interface, we have assumed in the derivation of Eq. (33) that $ze\psi < kT$, which implies that for a monovalent species,

$$\psi_0 < \frac{kT}{\varepsilon} = 25.7 \text{ mV} \tag{34}$$

assuming $T = 25°C$. Thus, to be rigorously correct, Eq. (33) is valid only for surface potentials less than approximately 25 mV. Later we shall check to see if this is a reasonable assumption for the case of typical capillary buffer systems used in CE.

Next, we should examine the physical significance of the constant κ in Eq. (33). From Eq. (32) we can see that for the term in the exponent to be dimensionless, κ must have the dimensions of inverse length. Therefore, κ^{-1} has the dimensions of length. Writing Eq. (32) in terms of κ^{-1},

$$\psi(x) = \psi_0 \exp\left(-\frac{x}{\kappa^{-1}}\right) \tag{35}$$

From Eq. (35) it can be seen that when $x = \kappa^{-1}$, $\psi = \psi_0/e$. For this reason κ^{-1} is called the double-layer "thickness." See Figure 7. Because κ^{-1} is such an important parameter, it is helpful to express it in terms of ionic concentrations rather than number densities, as is done in Eq. (30). In terms of ionic concentrations in moles per liter, C_i, assuming that n_i has units of (number of ions)/m^3,

$$n_i = 1000\, N_A\, C_i \tag{36}$$

where N_A is Avogadro's number. Thus, Eq. (30) becomes

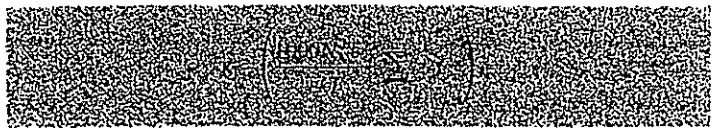

(37)

Note that the summation in Eq. (37) is equal to twice the ionic strength of the solution. Hiemenz (1986) provides a convenient table of values of κ based on Eq. (37) for aqueous electrolyte solutions at 25°C as a function of electrolyte concentration and valence. This table is reproduced in Table I.

Finally, it is sometimes helpful to express Eq. (33) in terms of surface charge density, σ^*, rather than surface potential, ψ_0. Based on the requirement for electroneutrality, the total charge on the capillary wall must equal the total charge in the solution, therefore

$$\sigma^* = \varepsilon \int_0^\infty \rho(x)dx \tag{38}$$

Table I Values[a] of the Electrical Double-Layer Thickness, κ^{-1}

Molarity of electrolyte	Symmetrical electrolyte		Asymmetrical electrolyte	
	$Z^+:Z^-$	κ^{-1} (m) · 10^9	$Z^+:Z^-$	κ^{-1} (m) · 10^9
0.001	1 : 1	9.61	1 : 2, 2 : 1	5.56
	2 : 2	4.81	3 : 1, 1 : 3	3.93
	3 : 3	3.20	2 : 3, 3 : 2	2.49
0.01	1 : 1	3.04	1 : 2, 2 : 1	1.76
	2 : 2	1.52	1 : 3, 3 : 1	1.24
	3 : 3	1.01	2 : 3, 3 : 2	0.787
0.1	1 : 1	0.961	1 : 2, 2 : 1	0.556
	2 : 2	0.481	1 : 3, 3 : 1	0.393
	3 : 3	0.320	2 : 3, 3 : 2	0.249

[a] For different electrolyte concentrations and valences for aqueous solutions at 20°C. Values are calculated using Eq. (36).

Combining Eqs. (28) and (38) results in an expression relating ψ and σ^*,

$$\sigma^* = \varepsilon \int_0^\infty \frac{d^2\psi}{dx^2}\, dx \tag{39}$$

Performing the integrations using the boundary conditions: (1) $x = \infty$ when $d\psi/dx = 0$; (2) $x = 0$ when $\psi = \psi_0$, gives

$$\sigma^* = \varepsilon\kappa\psi_0 \tag{40}$$

Thus, Eq. (40) provides a relationship between the surface charge density and the electrical potential at the surface of the capillary in a given electrolyte solution. Therefore, in terms of surface charge density, Eq. (33) becomes

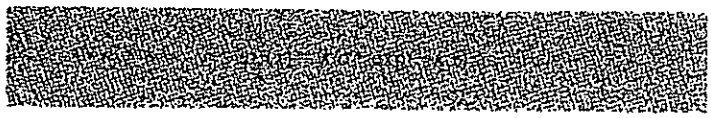

(41)

Now that we have a quantitative relationship describing $\rho_e(x)$, we can determine the electroosmotic velocity profile.

B. Electroosmotic Velocity Profile

In this section we derive the velocity profile for electroosmotic flow. The nature of this profile is one of the key reasons for the very high separation efficiencies (or low dispersion) possible in CE separations. This problem was first solved by Rice and Whitehead (1965) for flow in cylindrical capillaries. This presentation will follow closely that of Rice. However, to improve the clarity of the treatment, we shall perform the derivation in rectangular rather than cylindrical coordinates. As we shall see, this will not affect the final conclusions of the analysis.

The equation which relates the forces on a fluid to its velocity profile is the equation of motion (Fahien, 1983). The equation of motion for a Newtonian electrolyte solution, flowing in one dimension across a flat surface, under the influence of an electric field in the direction of flow, is

$$\eta \frac{d^2 v_z(x)}{dx^2} E\rho_e(x) \tag{42}$$

where η is the viscosity of the solution, v_z is the fluid velocity in the z direction and E is the electrical field strength. To solve Eq. (42) for $v_z(x)$, we simply integrate Eq. (42) twice using the boundary conditions: (1) $dv/dx = 0$ at $x = \infty$; (2) $v_z(x) = 0$ at $x = 0$. The result is

$$v_z(x) = \frac{-E\varepsilon\psi_0}{\eta}(1 - \exp(-\kappa x)) \tag{43}$$

The key feature of Eq. (43) is the fact that for typical values of κ and x used in CE, the exponential term quickly vanishes. At this point we can calculate how far away from the capillary wall the fluid velocity reaches its constant value of v_{∞}. Substituting Eq. (40) into Eq. (43) gives

$$v_z(x) = \frac{-E\sigma^*}{\kappa\eta}(1 - \exp(-\kappa x)) \tag{44}$$

If we assume that the wall of a fused-silica capillary has a charge density of 0.01 C/m^2 (Churaev *et al.*, 1981) and that $\kappa = 3.29 \cdot 10^8$ m^{-1} (see Table I), we can calculate $v_z(x)$. In Fig. 8, Eq. (44) is plotted for the case where E = 30,000 V/m and η = 0.001 N sec/m^2. As can be seen in Fig. 8, the velocity does indeed reach a constant value very close to the capillary wall. In fact, within 14 nm of the capillary wall, $v_z(x) = 0.99v_{\infty}$. Therefore, in a 50-μm inside diameter (i.d.) capillary, $v_z(x) = v_{\infty}$ across 99.95% of the capillary cross-section. Thus the assumption of a flat, radially independent velocity profile appears to be justified.

Therefore, given that the exponential term in Eq. (43) can be neglected, Eq. (43) reduces to

$$v_z(x) \approx v_{\infty} = \frac{-E\varepsilon\psi_0}{\eta} \tag{45}$$

where v_{∞} is the velocity of the fluid far away from the influence of the capillary wall. In terms of the electroosmotic mobility, i.e., the electroosmotic velocity per unit elec-

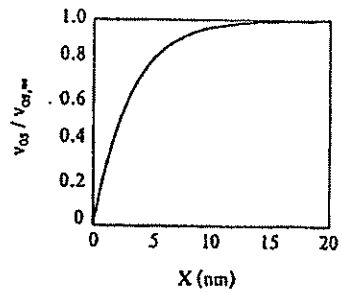

Figure 8 Calculated values of the electroosmotic velocity, v_{os}, as a function of the distance from the capillary wall, x, where $v_{os,\infty}$ is the fluid velocity in the bulk solution. This curve was evaluated using Eq. (45) where E = 30,000 V/m, $\kappa = 3.29 \cdot 10^8$ m, and $\sigma^* = 0.01$ C/m^2. From Churaev *et al.* (1981).

trical field strength, Eq. (45) becomes

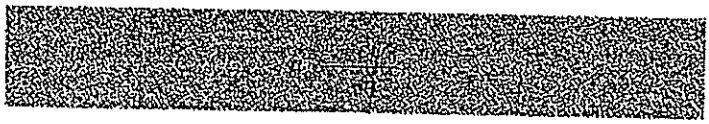

(46)

The striking feature of Eq. (45) is that it says that the velocity of the fluid is *not a function of radial position.* This is in contrast to the case of pressure-driven flow where the well-known parabolic velocity profile is present. This "flat" velocity profile makes possible the very low dispersion found in CE separations. Clearly, because v_x is independent of the distance from the solid surface, it makes no difference that we performed the analysis in rectangular coordinates.

At this point, we are in a position to perform some calculations to help gain a quantitative feel for these effects. For example, how do predicted values of the electroosmotic mobility, μ_{os}, compare with typical measured values? Substituting Eq. (40) into Eq. (46) gives

$$\mu_{os} = \frac{\sigma^*}{\kappa \eta} \tag{47}$$

Using the same values for σ, κ, and η as in the previous example gives us a value for μ_{os} of $6.1 \cdot 10^{-8}$ m^2/V · sec. Given that the value for σ was measured at a pH of 7.1, it can be seen from Fig. 9 that the calculated value of μ_{os} agrees with experimental observations.

Next, we can see if the potential at the surface of the capillary, ψ_0, lies within the limits of the Debye-Hückel approximation. Given experimental values for μ_{os} and Eq. (46), we can obtain a direct measure of ψ_0.

$$\psi_0 = \frac{v_{ss}\eta}{E\varepsilon} = \frac{\mu_{os}\eta}{\varepsilon} \tag{48}$$

Given that the electrical permittivity of water at 25°C is $6.95 \cdot 10^{-10}$ C^2/J · m, according to Eq. (48), ψ_0 = 86 mV. Although this is larger than the 25-mV limit stated for the Debye-Hückel approximation, the error introduced by this slightly higher value of ψ_0 does not appreciably affect the results of this analysis.

Finally, we can find out how the magnitude of the volumetric flow rate caused by electroosmosis compares to that caused by a pressure gradient. The volumetric flow rate due to electroosmosis, Q_{os}, is related to the electroosmotic mobility by

$$Q_{os} = v_{ss} S = \mu_{os} E S \tag{49}$$

where S is the cross-sectional area of the capillary. Using the same values as before for μ_{os} and E, Eq. (49) gives a value for Q_{os} of $3.53 \cdot 10^{-12}$ m^3/sec or 3.53 nl/sec. To calculate the volumetric flow rate due to a pressure gradient, we can use the Poiseuille

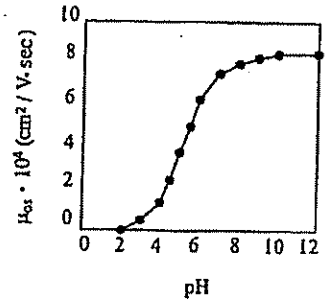

Figure 9 Dependence of electroosmotic mobility, μ_{os}, on buffer pH for the case of a fused-silica capillary that has been prewashed with 1.0 *M* NaOH. Reprinted with permission from Applied Biosystems (1990).

equation (Fahien, 1983),

$$Q = \frac{\pi \Delta P R_i^4}{8 L_{tot} \eta} \tag{50}$$

where ΔP is the pressure drop across the capillary and L_{tot} is its length. Thus, to generate a flow of $3.53 \cdot 10^{-12}$ m^3/sec would require a $\Delta P/L$ of $2.3 \cdot 10^4$ N/m^2/m or 3.4 psi/m. Thus, for this example, with regard to volumetric flow rate, an electrical potential of 30,000 V/m is comparable to a pressure gradient of 3.4 psi/m.

C. Control of Electroosmosis

For many applications it is desirable to be able to manipulate the magnitude of the electroosmotic flow in order to optimize separation performance. Many studies have been conducted describing various methods that can be used to control electroosmotic flow.

In order to control electroosmosis, it is clear from Eqs. (46) or (47) that one must control either the charge density on the capillary wall, the double-layer thickness, or the viscosity of the solution adjacent to the capillary wall. This can be clearly seen if we express Eq. (47) in terms of the double-layer thickness, κ^{-1},

$$\mu_{os} = \frac{\sigma^* \kappa^{-1}(\varepsilon, C_i)}{\eta} \tag{51}$$

where the dependence of κ^{-1} on ε and C_i has been indicated. Therefore, each of the techniques that follow acts by affecting one or the other of these parameters.

Two approaches have been used to control μ_{os} by reducing the double-layer

thickness, κ^{-1}. The first simply uses an increased concentration of electrolytes in the electrophoresis buffer. As can be seen in Eq. (37), this will serve to reduce κ^{-1}. Detailed studies of the effect of varying NaCl concentration on μ_{os} have been reported (Fujiwara and Honda, 1986). A drawback to this approach is that the increased ion concentration will increase the amount of Joule heating within the capillary, thus potentially affecting separation performance. A second approach is to decrease κ^{-1} by decreasing the permittivity of the buffer by the addition of simple organic solvents. Again from Eq. (37), it can be seen that as ε is decreased, κ^{-1} will become smaller. Organic solvents that have been investigated include acetonitrile and methanol (Fujiwara and Honda, 1987). A potential drawback to using organic solvents in the electrophoresis buffer is the large ultraviolet (UV) absorbance background associated with these solvents, which could negatively affect detection sensitivity while using a UV-absorbance detector.

Three main approaches have been examined to control μ_{os} by influencing the surface charge density on the capillary wall, σ^*. The first uses physically adsorbed small cationic molecules to neutralize the charge on the capillary wall. Molecules that have been used for this purpose include cetyltrimethylammonium bromide (Altria and Simpson, 1986), tetradecyltrimethylammonium bromide (Huang *et al.*, 1989), putrescine (Lauer and McManigill, 1986a), and *s*-benzylthiouronium chloride (Altria and Simpson, 1987). Using multivalent ions, one can even reverse the *direction* of the electroosmotic flow using this method (Wiktorowicz and Colburn, 1990). A drawback to this approach is that the cations can potentially bind to the analyte molecule, changing its net charge and thus its electrophoretic mobility. A second approach to influence σ^* is to covalently block the charged silanol groups on the capillary surface. Chemical derivitizing agents that have been used for this purpose include trimethylchlorosilane (Jorgenson and Lukacs, 1983) and (γ-methacryloxypropyl)-trimethoxy silane (Hjertén, 1985). A study of the effect of a number of silanating reagents is given by McCormick (1988). A drawback to this approach is that over time, the covalent bond can hydrolyze, thus allowing the blocking agent to leach off the surface of the capillary, contaminating the buffer and causing μ_{os} to change over time. A third approach used to manipulate σ^* is simply to titrate the charge on the capillary surface. The point of zero charge for fused silica has been found to be approximately at a pH of 2.0 (Churaev *et al.*, 1981). As can be seen from the titration curve in Fig. 9, this does indeed appear to be the case. An obvious drawback of this approach is that if, at the desired pH, the analyte molecule is oppositely charged, a significant amount of interaction between the analyte and the wall can result. However, this method has been effectively exploited for peptide separations at a pH of 2.5 without any apparent wall sticking (Grossman *et al.*, 1989).

The last parameter that can be used to alter μ_{os} according to Eq. (51) is η, the solution viscosity. By adding to the buffer a polymer which adsorbs to the capillary wall, one is able to greatly increase the effective viscosity of the buffer near the capillary–buffer interface. The use of a number of different noncovalently bound polymers for this purpose has been investigated by Herrin *et al.* (1987).

CHAPTER 4

Free-Solution Capillary Electrophoresis

Paul D. Grossman

I. Introduction

As is the case for all electrophoretic separations, in free-solution capillary electrophoresis (FSCE), separations are achieved as a result of the unequal rate of migration of different solutes under the influence of an externally applied electric field. However, FSCE differs from the other modes discussed in this book in one important respect — there is no secondary influence, other than the structure of the analyte and the solvent, contributing to the selectivity of the separation. There is no polymer network, superimposed pH gradient, or secondary phase.

Because the analyte is typically not chemically altered before the analysis, FSCE is a direct analog to native gel or paper electrophoresis. However, because there is no solid support, in the case of FSCE there are no *matrix* effects; thus, FSCE is well suited to detect subtle changes in the structure of native macromolecules.

In this chapter, we review the factors that determine the electrophoretic mobility of a solute as measured by FSCE and briefly discuss the dispersive phenomena that, along with differences in the electrophoretic mobility, dictate the resolving power of the technique. In addition, we discuss practical aspects of FSCE measurements, and some experimental studies that use model systems to explore the various factors determining selectivity in FSCE.

Capillary Electrophoresis

II. Electrophoretic Mobility

A. Definition of the Electrophoretic Mobility

When a charged particle is placed in an external electric field, E, it experiences a force, F_e, which is equal to the product of its net charge q, and the electrical field strength, E,

$$F_e = q \cdot E \tag{1}$$

In addition to the electrical force acting on the particle, once it begins to move, the particle experiences a drag force in the direction opposite to its direction of motion. This drag force, F_d, is proportional to the particle velocity,

$$F_d = f \cdot v \tag{2}$$

where the proportionality constant f is called the translational friction coefficient. For example, for a spherical particle, f is given by Stokes' law as

$$f = 6\pi\eta R \tag{3}$$

where η is the viscosity of the surrounding medium, and R is the apparent hydrodynamic radius of the particle. Thus, the equation describing the translational motion of a particle under the influence of an electric field is

$$m\left(\frac{dv}{dt}\right) = qE - fv \tag{4}$$

where m is the mass of the particle.

Except for a brief transient when the electrical force is first applied, the electrostatic force is exactly counterbalanced by the drag force, resulting in a steady state velocity, v_{ss}. Typically, for macromolecules, this transient is very short, on the order of 10^{-11} sec. By equating Eqs. (1) and (2), the resulting steady-state velocity can be related to the charge and frictional properties of the particle by the simple relationship

$$v_{ss} = \frac{qE}{f} \tag{5}$$

Furthermore, the electrophoretic mobility, μ, of a particle is defined as the steady-state velocity per unit field strength, or, from Eq. (5),

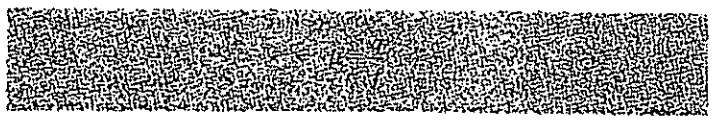

(6)

Clearly, differences in the electrophoretic mobility of molecules can arise as a result of differences in frictional properties, i.e., size or shape, or as a result of differences in the net charge on the molecule. These differences in the properties of molecules form the basis for the selectivity in FSCE separations. We shall discuss the relationship between the molecular structure and the electrophoretic mobility of an analyte in the following subsections.

B. Relationship between Mobility and Molecular Size

The way in which the frictional coefficient, f, is related to the size of a molecule depends on what model is used to describe the conformation of the molecule and on the nature of the solvent. In this section we discuss the case of a solute migrating through free solution.

If, in free solution, the migrating molecule is modeled as a solid sphere, the relationship between the translational frictional coefficient and molecular size would be straightforward. From Stokes' law we know that

$$f = 6\pi\eta R \tag{7}$$

Furthermore, for a solid sphere, the radius and the mass, m, are related by

$$m = \rho_p\left(\frac{4}{3}\pi R^3\right) \tag{8}$$

where ρ_p is the density of the particle. Thus,

$$R \sim m^{1/3} \tag{9}$$

where the "~" symbol indicates proportionality. Therefore, from Eqs. (6) and (9)

$$f \sim m^{1/3} \tag{10}$$

If, rather than being a solid sphere, the solute behaves as a loose coil or a rod, we can no longer use Eq. (8) to directly relate the molecular mass to an apparent hydrodynamic radius and thus to a value for f. However, the relationship between mass and the translational friction coefficient has been established for a number of practically important molecular conformations. Some of these are given in Table I. Table I clearly shows that the way in which electrophoretic mobility in free solution is related to molecular size is strongly dependent on the model chosen to represent the conformation of the solute.

Table I Proportionality Relationship between Frictional Coefficient and Molecular Weight[a]

Molecular model	Proportionality relationship
Solid sphere	$f \sim (MW)^{1/3}$
Random coil — unperturbed chain	$f \sim (MW)^{0.5 \text{ to } 0.6}$
Long rod	$f \sim (MW)^{0.8}$
Wide thin disk	$f \sim (MW)^{2/3}$
Free-draining coil	$f \sim (MW)^{1.0}$

[a] Reproduced with permission from Cantor and Schimmel (1980).

APP 215980

B 18

As it turns out, for many practically important applications, DNA and sodium dodecyl sulfate (SDS)-treated protein applications in particular, separations based solely on differences in free-solution electrophoretic mobilities are not possible. This is a direct result of the relationship between f and the molecular size characteristic of these solutes. This can be demonstrated through a simple argument, using DNA as an example.

The structure of the DNA molecule is such that the total net charge on the molecule is directly proportional to its size; i.e., approximately two charges per base pair. Thus,

$$q \sim N \tag{11}$$

where N is the number of units (base pairs) in the DNA chain. In addition, since DNA exists in solution as a free-draining coil, it can be seen from Table I that

$$f \sim N \tag{12}$$

(A free-draining coil is one in which each of the units of the chain contributes equally to the overall drag of the chain.) Finally, by combining Eqs. (11) and (12) with the definition for electrophoretic mobility, Eq. (6), it can be seen that μ is no longer a function of molecular size, i.e.,

$$\mu = \frac{q}{f} \sim \frac{N}{N} = N^0 \tag{13}$$

where N^0 indicates that μ is constant with respect to changes in N. Thus, because both the charge and the frictional drag are proportional to molecular size, free-solution electrophoretic separations of DNA are impossible. This argument also applies to the case of SDS proteins in which charge is also directly proportional to N, and the polymer behaves as a free-draining coil. Therefore, in order to perform a separation of DNA fragments, or of any molecule with a constant ratio of net charge to translational friction coefficient, one must exploit an alternate separation mechanism. If, instead of allowing the DNA molecule to migrate in free solution, one forces it to travel through a porous polymer network, one can impart a size dependence to the electrophoretic mobility. The migration of chainlike molecules through a polymer network will be discussed in Chapter 8.

C. Effect of Buffer Ions on the Effective Charge and Mobility

1. Charge Screening

In an electrolyte solution, when a charged solute is moving, the effective charge of the solute, q, is less than the total charge, owing to the screening influence of the counterions in solution. This shielding is attributable to the presence of counterions located within a stagnant layer immediately adjacent to the surface of the solute (see Fig. 1). The stagnant layer is caused by the viscous force acting between the solvent and the surface of the solute. The interface between the stagnant layer and the surrounding solution is called the surface of shear. The exact position of the surface of shear is not

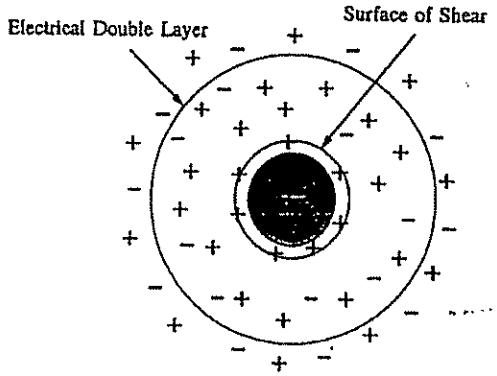

Figure 1 Schematic illustration of the ion atmosphere surrounding a negatively charged spherical particle.

known, but typically it is assumed that it has a thickness on the order of a few molecular diameters.

As might be expected, the degree of counterion shielding depends on the nature and concentration of the counterions as well as properties of the solvent and the analyte. The complete general description of this phenomenon is complex and beyond the scope of this chapter. However, in order to gain an appreciation of the key features of this effect, we shall explore a simplified case — that of a "small" spherical particle in a dilute electrolyte solution, where the thickness of the counterion atmosphere is large compared to the radius of the solute particle.

From elementary physics, we know that the electrostatic potential, ψ, at a distance r from the surface of a uniformly charged sphere of radius R and total charge q in a medium having a permittivity of ε is (Atkins, 1978)

$$\psi(r) = \frac{q}{4\pi\varepsilon r}; \qquad r > R \tag{14}$$

To find an expression for the effective charge of the same charged sphere in an electrolyte solution, we will first determine the effect of the ions on $\psi(r)$ and then compare the resulting expression with that of Eq. (14). This discussion will follow closely that of the electrical double layer presented in Chapter 1. However, in this case, spherical rather than planar coordinates will be used.

To determine the electrostatic potential in the vicinity of a charged spherical solute in an electrolyte solution, we must solve Poisson's equation in cylindrical coordinates,

$$\frac{1}{r^2}\frac{d}{dr}\left(r^2\frac{d\psi}{dr}\right) = \frac{-\rho^*}{\varepsilon} \tag{15}$$

APP 215982

B 20

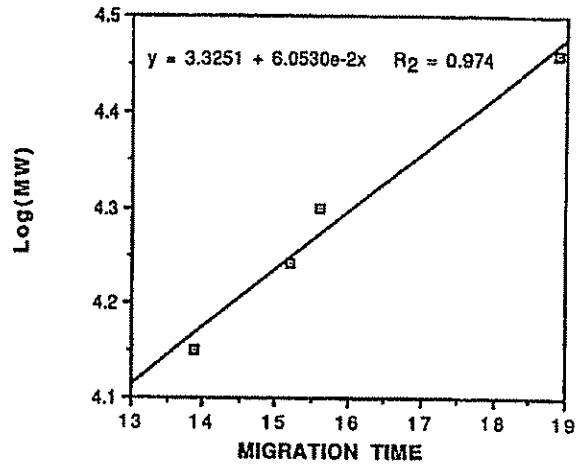

Figure 7 The log of the molecular weight is plotted versus migration time for the electropherogram in Fig. 6.

SDS capillary gel electrophoresis shows potential as a useful analytical tool for the molecular weight determination of proteins. There are, however, several hurdles that must be overcome to make this technique truly viable. The first is that gels must be devised that do not absorb in the 200-nm range, or off-column detection methods must be developed so that sensitivity and quantitative accuracy can be improved. In addition, SDS interacts with most water-soluble polymers, causing instability in the gel matrix and limiting field strengths. Consequently, analysis times are increased, thus dropping sample throughput below that of slab-gel electrophoresis. Resolution using capillary gels appears to be roughly equivalent to that in slab-gel techniques, reducing the incentive to change formats. Improvements in these three areas will make capillary gel electrophoresis a powerful protein analysis tool.

B. Oligonucleotide Analysis

Capillary gel electrophoresis is an efficient technique for directly analyzing the purity of synthetic oligonucleotides (Dubrow, 1991). Methods have been devised in the various disciplines of chemical synthesis to determine the purity of reagents. It would be almost unheard of today to buy a specialty chemical without knowing its purity. For the millions of synthetic oligonucleotides produced annually, purity is not generally determined due to the need to use labor intensive classical techniques such as slab gel electrophoresis or the inability of high-pressure liquid chromatography to deliver adequate resolution.

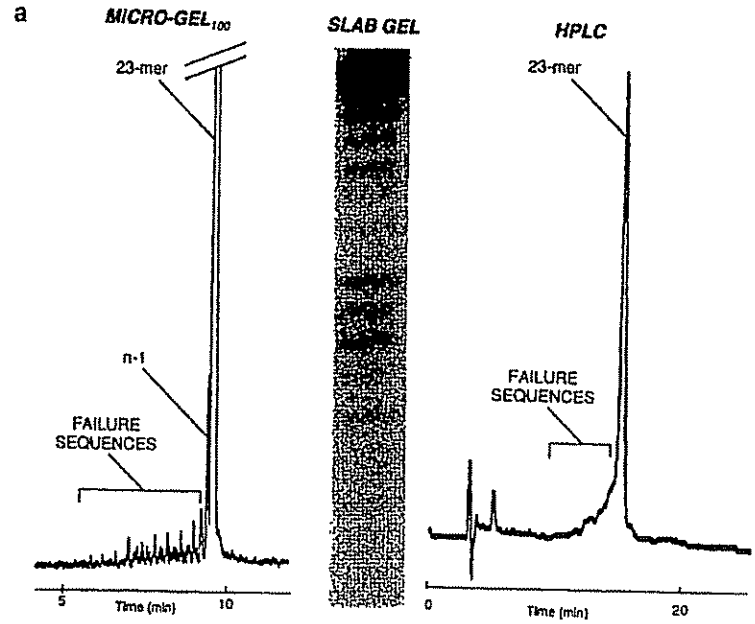

Figure 8 Random sequence oligonucleotides 23 (a), 40 (b), and 120 (c) bases in length were analyzed by capillary gel electrophoresis, slab-gel electrophoresis and HPLC (owing to poor resolution, the 120-mer analyzed on HPLC is not shown). Conditions for capillary gel runs were field strength, 300 V/cm; temperature, 30°C; 30 cm effective separation length; detection wavelength, 260 nm; 75 m*M* pH 7.6 Tris-phosphate buffer was used with a MICRO-GEL$_{100}$ gel-filled capillary. Slab gels were 20 × 40 × 0.4 cm, 20% polyacrylamide, contained 90 m*M* Tris-borate and 7 *M* urea, and were run at 50 mA constant current. The HPLC runs were made on a reverse-phase column with a triethylacetate versus acetonitrile gradient. Detection was performed at 260 nm. *(Figure continues.)*

Figure 8 compares separations of three synthetic oligonucleotides, a 23-, 40-, and 120-mer, by capillary gel electrophoresis, ^{32}P slab-gel electrophoresis, and reverse-phase HPLC. Attempts to analyze the 120-mer by HPLC were unsuccessful, owing to poor resolution (data not shown).

Comparison of the three methods yields the following conclusions:

1. Gel-filled capillaries can provide high resolution up to and beyond 120 bases. This range covers essentially all synthetic oligonucleotides currently produced.
2. One gel concentration can effectively cover the entire range of synthetic oligonucleotides.

for the electro-

lytical tool for
veral hurdles
hat gels must
tion methods
improved. In
tability in the
are increased,
Resolution us-
echniques, re-
eas will make

ng the purity
ed in the vari-
It would be
s purity. For
not generally
h as slab gel
y to deliver

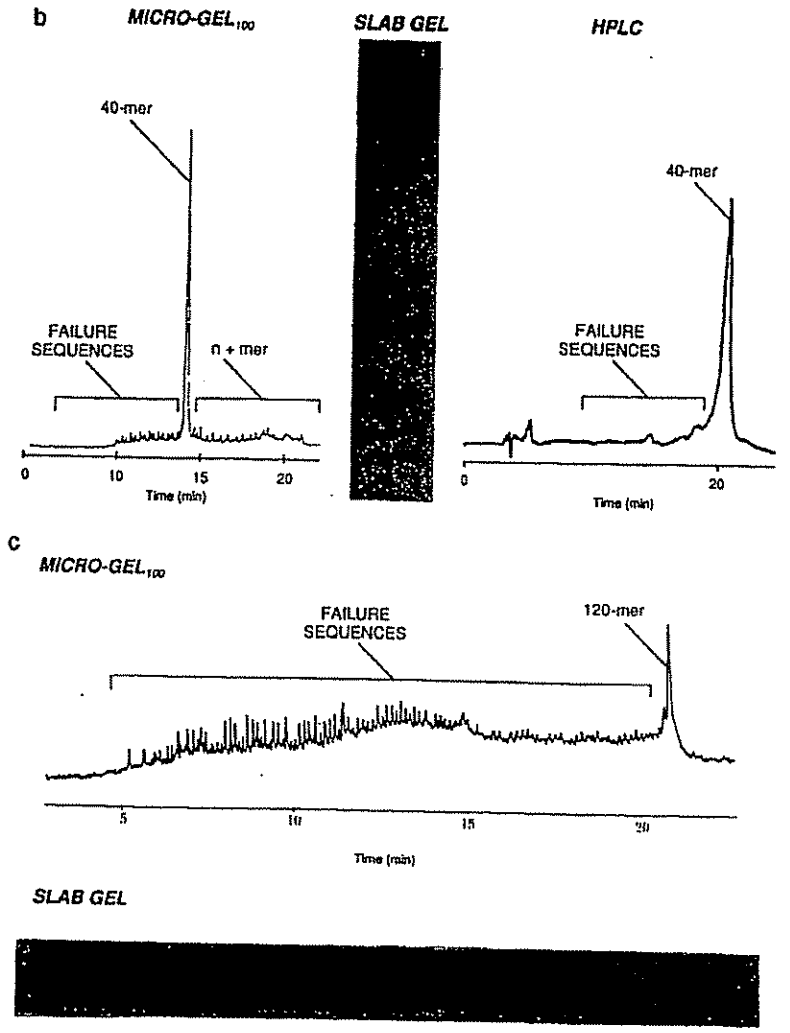

Figure 8 *(Continued)*

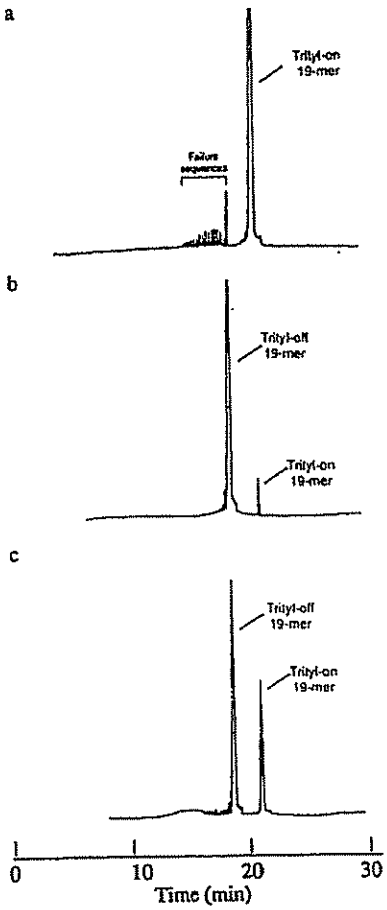

Figure 9 Electropherograms of a 19-base oligonucleotide in its (a) crude trityl-on state, (b) purified trityl-off state, and (c) as a mixture of (a) and (b). Field strength for each run was 300 V/cm; temperature, 30°C; 30 cm effective separation length; detection wavelength, 260 nm;75 m*M* pH 7.6 Tris-phosphate buffer was used with a MICRO-GEL$_{100}$ gel-filled capillary.

3. Both capillary gel and slab-gel electrophoresis provide higher resolution than HPLC. For HPLC analysis, resolution is limited to 40 bases or less (Baba *et al.*, 1991). Below 40 bases resolution is significantly poorer than with either gel technique.
4. Detection and data collection with capillary gel electrophoresis is quantitative and done in real time, providing rapid results. Slab-gel detection methods are indirect, requiring staining or radioactive labeling and developing.
5. Capillary gel electrophoresis can analyze samples in minutes, for rapid throughput of critical samples.

Capillary gel electrophoresis can also be used to evaluate the removal of dimethoxytrityl (DMT)-protecting groups from the ends of synthetic oligonucleotides. Complete detritylation is required for the successful use in cloning or ligation experiments and for the use in experiments that require labeling of the oligonucleotide. The trityl-containing species runs significantly slower than the deblocked oligonucleotide. This can be clearly seen in Fig. 9, where electropherograms of a trityl both on and off electropherogram are presented, along with a mixture of the two species.

Oligonucleotides with phosphorylated or dephosphorylated 5′ ends can also be easily detected by capillary gel electrophoresis (Fig. 10). The dephosphorylated species runs slower than the more highly charged phosphorylated oligonucleotide. Clearly, capillary gel electrophoresis can provide a simple and rapid assay for phosphorylation, which often determines biological activity of an oligonucleotide.

Similar to that with slab-gel electrophoresis (Efcavitch, 1991), relatively short oligonucleotides will exhibit a base composition dependence with respect to migration time. Figure 11 shows the electropherogram of a mixture of 12-base-long polyoligodeoxyadenylic acid (pdA_{12}), polyoligodeoxythymidylic acid (pdT_{12}), and polyoligodeoxycytidylic acid (pdC_{12}). The order of migration is

$$A > T > C$$

Polyoligodeoxyguanylicacid (pdG) runs considerably slower than pdC, as would be predicted from traditional slab-gel results.

If an internal reference standard of known concentration is included when a crude oligonucleotide sample is prepared for analysis, the synthesis yield can be calculated directly from the electropherogram by determining the ratio of the reference peak to the product peak. This promises to be much more informative than the widely used method of measuring the absorbance of the entire crude product, including failure sequences and impurities, against a reference on a UV spectrophotometer (Fig. 12).

Gel concentrations ranging from 10% T/0% C (Heiger *et al.*, 1990) to 5% T/3% C (Lux *et al.*, 1990) have been used effectively to separate oligonucleotides. Generally Tris-borate buffers containing 7 *M* urea have been used, although Tris-phosphate has also been used (Applied Biosystems, 1990). Detection is performed using UV absorption at 260 nm.

Sample concentrations between 4 μg/ml and 0.6 μg/ml in water or denaturant solution are typically used. Dilutions from crude synthesis mixtures containing ammo-

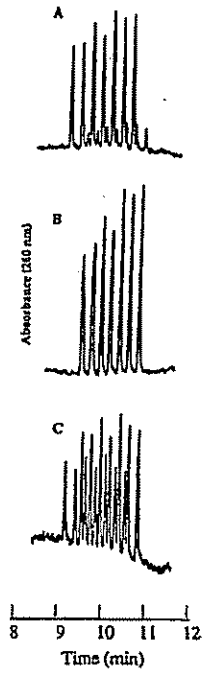

Figure 10 Comparative electropherograms of a $(dA)_{12-18}$ oligonucleotide ladders run on a gel-filled capillary with (A) the oligonucleotides phosphorylated at the 5′ hydroxy end, (B) the oligonucleotides dephosphorylated, and (C) a mixture of the phosphorylated and dephosphorylated ladders. Field strength for each run was 300 V/cm; temperature, 30°C; 30 cm effective separation length; detection wavelength, 260 nm; 75 m*M* pH 7.6 Tris-phosphate buffer was used with a MICRO-GEL$_{100}$ gel-filled capillary.

nia in deionized water can be injected directly onto the capillary without any intermediate steps. Capillary gel electrophoresis appears to be an efficient method for the analysis of synthetic oligonucleotides. Its combination of ease of use, speed, resolution, and quantitation should make this technique a fixture in synthetic oligonucleotide laboratories.

C. DNA Sequencing

It has been shown that fluorescent-labeled DNA fragments generated in an enzymatic sequencing reaction can be rapidly separated by capillary gel electrophoresis and detected at attomole levels within the capillary (Drossman *et al.*, 1990; Swerdlow and

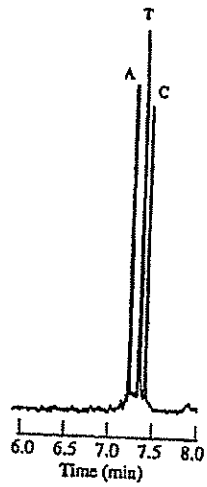

Figure 11 A mixture of four oligonucleotide homopolymers, dA_{20}, dT_{20}, and dC_{20} of equal length were analyzed by capillary gel electrophoresis. Field strength for each run was 400 V/cm; temperature, 30°C; 30 cm effective separation length; detection wavelength, 260 nm; 75 m*M* pH 7.6 Tris-phosphate buffer was used with a MICRO-GEL$_{100}$ gel-filled capillary.

Gesteland, 1990). A great deal of interest has been focused on this technique in the hope that it might be the cornerstone of a high-speed genomic sequencer.

Current capillary sequencers utilize an argon laser source that is focused onto a capillary, causing excitation of the fluorescent-tagged DNA. The emission is sent through a bandpass filter to select the wavelength region of interest and then detected with a photomultiplier tube, electronically filtered, digitized, and stored on a computer for analysis. Multiple bandpass filters can be used, along with a beam splitter, to detect different labels simultaneously (Drossman *et al.*, 1990). Off-column detection by a sheath flow method has also been used effectively (Swerdlow and Gesteland, 1990).

Polyacrylamide gel concentrations of about 3% T and 5% C seem to be most widely used. Higher concentrations appear to blur longer fragments. Linear acrylamide gels have also been used by Heiger *et al.* (1990) for sequencing. Tris-borate buffers containing 7 *M* urea have been used exclusively to date for sequencing.

With capillary diameters of typically 50 μm compared to those of slab gels of 300 μm, the time to determine the sequence of a DNA fragment can be reduced by a factor of five to ten. However, unless a relatively simple and cost-effective method for running multiple capillary separations simultaneously is devised, the time per sequenced base on an automated slab gel sequencer is a factor of three faster, since up to 24 lanes can be run simultaneously. The feasibility of ultra-thin (50-μm) slab-gel sequencers is being investigated and may prove to be the optimal format using tradi-

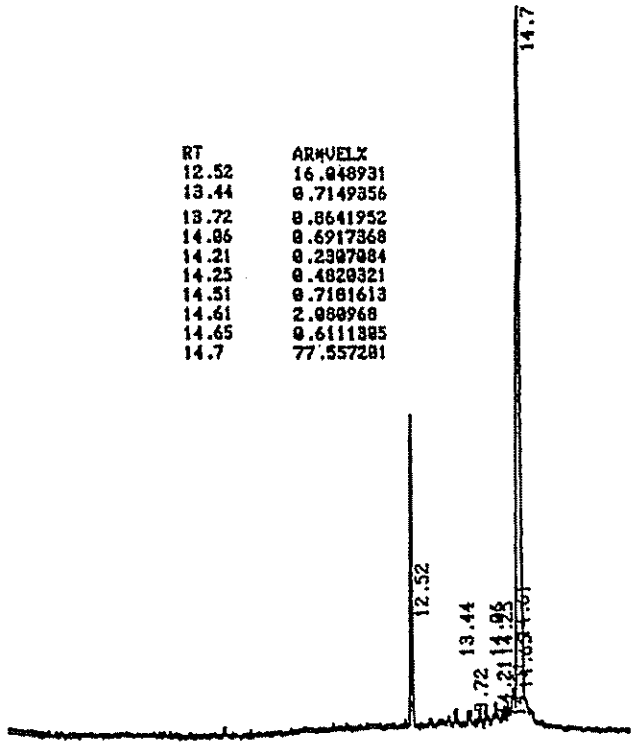

Peak Area(%)		Peak Ratio#	Concentration(O.D.)	
$d(A)_{12}$	$(AGTC)_6$	$d(A)_{12}/(AGTC)_6$	$d(A)_{12}$	$(AGTC)_6$
15.8	74.76	0.2117	0.10	0.47

Figure 12 An electropherogram of a mixture of a crude synthetic (5′-AGCTAG CTAGCT AGCTAG CTAGCT-3′) oligonucleotide and an oligonucleotide marker (pdA_{12}) of known concentration. By determining the area ratio of the two peaks, the concentration of $(AGCT)_6$ is determined. Field strength for each run was 300 V/cm; temperature, 30°C; 30 cm effective separation length; detection wavelength, 260 nm; 75 m*M* pH 7.6 Tris-phosphate buffer was used with a MICRO-GEL_{100} gel-filled capillary.

nd dC_{20} of equal each run was length, 260 nm. capillary.

hnique in the

focused onto a mission is sent then detected on a computer litter, to detect tection by a land, 1990).

n to be most near acrylam- g. Tris-borate ncing.

slab gels of e reduced by ective method he time per ster, since up μm) slab-gel using tradi-

tional gels, however, capillary sequencing may show significant advantages in the area of resolution in the future. Current research has utilized conventional acrylamide gels, and resolution has been comparable to that with traditional sequencing results. Moving into novel gel materials made possible by the capillary format could have profound scientific implications, if larger fragments can be sequenced.

D. Double-Stranded DNA

Excellent separations of double-stranded DNA have been performed with gel-filled capillaries (Fig. 13). The most impressive work to date has been the use of a capillary filled with 3% T, 0.5% C acrylamide to base-line separate a DNA ladder from 71 to 12,000 bases (Heiger *et al.*, 1990). With the combination of speed, high resolution, and wide separation range, gel-filled capillary electrophoresis should find widespread use in evaluating the growing number of polymerase chain reaction (PCR) products for size and concentration.

As was mentioned in Section III,D, electrophoretic separations of double-stranded DNA have been accomplished in dilute polymer solutions. Hydroxylated cellulose derivatives have been widely used, generally in the concentration range of 0.1% to 1.0% (Chin and Colburn, 1989). With this technique the polymer solution can be drawn into the capillary under vacuum and subsequently rinsed out and replaced if necessary. This eliminates the problems associated with void formation and subsequent electrical failures in gel-filled capillaries. This technology is covered in depth in Chapter 8.

E. Chiral Molecules

Complexing agents have been incorporated into gel-filled capillaries to carry out stereospecific separations. The addition of β-cyclodextrin to polyacrylamide gel-filled capillaries has been shown to be effective in accomplishing electrophoretic separations of dansylated amino acids (Guttman *et al.*, 1988; Smith, 1990). Figure 14 shows an example of a separation of dansylated amino acids.

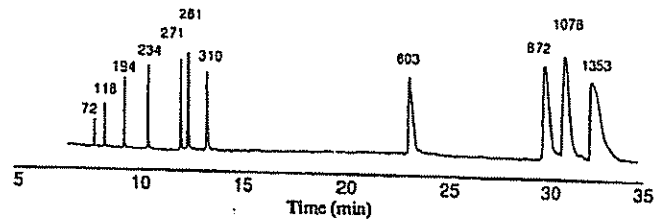

Figure 13 An electropherogram of oX174/*Hae* III restriction fragments separated on a gel-filled capillary is shown. Field strength for each run was 300 V/cm; temperature, 30°C; 30 cm effective separation length; detection wavelength, 260 nm; 75 m*M* pH 7.6 Tris-phosphate buffer was used with a MICRO-GEL$_{100}$ gel-filled capillary.

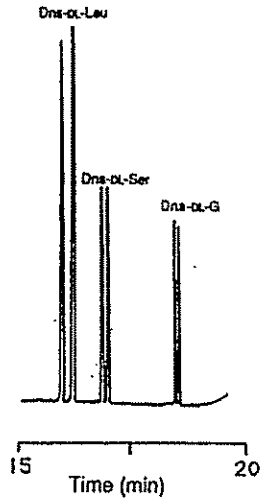

Figure 14 Separation of dansyl DL-isomers of leucine, serine, and glutamine on a gel-filled capillary containing β-cyclodextrin. Field strength was 300 V/cm; temperature, 30°C; 40 cm effective separation length; detection wavelength, 254 nm; Tris-borate pH 8.3 buffer was used, containing 7 *M* urea. A polyacrylamide gel was used in the capillary. From Smith (1990). Permission of Applied Biosystems.

Initially, chiral separations by capillary electrophoresis are being used to confirm HPLC separations. As research continues in this field, unique capabilities should be developed. Functionalization of the gel matrix with chiral agents is a particularly promising area.

V. Future Directions

The intensity of research and growing list of applications of capillary gel electrophoresis point to the potential of this technique to solve separations problems. The first wave of research has primarily focused on the challenge of reproducibly filling capillaries with polyacrylamide gels and optimizing their separations properties.

Capillaries based on this initial technology have reduced sample requirements and analysis times over existing separations methods. However, it is going to take a second wave of research that focuses on improved resolution and drives analysis times down to several minutes to realize the potential of capillary gel electrophoresis. This potential should be realized because of the geometrical advantage of the capillary, which opens the door to a variety of advanced separations materials.